Temperature-Memory Polymer Networks with Crystallizable Controlling Units

*Karl Kratz, Samy A. Madbouly, Wolfgang Wagermaier, and Andreas Lendlein**

Mechanically active polymers[1–8] and polymer composites[9–15] have attracted tremendous interest as thermosensitive materials because they are able to perform single,[16,17] dual,[6,10,15,18–20] or multiple[21–24] shape changes at predefined response temperatures (T_{sw}). In such polymer systems, T_{sw} is correlated to a thermal transition of the switching domains (T_{trans}), which is typically varied by adjusting the polymer's molecular structure (e.g., change in the switching segment length or chemical composition), and requires synthesis of a new material.[17,25–27] Recently, T_{sw} could be tailored for thermoplastic polymers and composites thereof with amorphous switching segments by variation of the temperature (T_{prog}) at which the sample was deformed before in order to memorize the shape change.[13,21,24,28–30]

Here we explored whether such a temperature-memory effect (TME) can be enabled for polymer networks with crystallizable controlling units. We designed temperature-memory polymers (TMPs) with high elasticity and a broad melting temperature range (ΔT_m) for the controlling unit. In contrast to the previously reported tunable amorphous polymers, here the crystallization process of the controlling units was manipulated in different ways, e.g., by cooling or by the application of strain. $T_{\sigma,max}$ is related to the stress maximum (σ_{max}) under constant strain activation conditions and T_{sw} of poly[ethylene-*ran*-(vinyl acetate)] (PEVA)-based TMP can be tailored over a wide temperature range up to 100 °C. These TMPs will substantially extend the spectrum of potential industrial applications for thermosensitive polymers, e.g., as low-cost, self-sufficient, reprogrammable release systems.

PEVA copolymers consist of crystallizable polyethylene segments and amorphous poly(vinyl acetate) segments. They comprise a relatively broad melting temperature T_m and two glass transition temperatures at –107 °C and –38 °C.[31] The T_m and the degree of crystallinity (DOC) can be influenced by variation of the VA content,[32] incorporation of crosslink,[33] or tensile drawing.[34] Based on the key requirements, high elasticity in combination with a broad ΔT_m, we selected a covalently crosslinked PEVA system as the entropy elastic copolymer network with crystallizable segments. A random sequence structure of the linear starting material ensures a broad chain segment length distribution resulting in a broad ΔT_m.

ΔT_m could be further extended to 100 °C by blending two PEVA copolymers containing different amount of crystallizable polyethylene segments and thus covering different ΔT_m ranges. PEVA91 with an ethylene content of 91 wt% (T_m = 102 °C, $\Delta T_m \approx$ 80 °C) and PEVA60 (60 wt% ethylene content; T_m = 55 °C, $\Delta T_m \approx$ 60 °C) were mixed and irregularly distributed covalent crosslinks were introduced by thermally induced radical crosslinking using dicumyl peroxide (DCP)[33,35] (see Experimental Section).

An almost complete network formation was confirmed for the crosslinked, binary blend c(PEVA91/PEVA60) by high values for the gel content (G) > 94% as determined in swelling experiments using chloroform (see Experimental Section). For c(PEVA91/PEVA60) an endothermic melting peak starting from 0 °C to 100 °C with a maximum at T_m = 96 °C was observed in differential scanning calorimetry measurements (see Supporting Information Method 3 and Supporting Information **Figure 1**).

The thermomechanical treatment, which we named the temperature-memory creation procedure (TMCP) was designed in such a way that the mechanical deformation (ε_m) is predominantly fixed by the volume fraction of the crystallites associated with a T_m close to T_{prog}. Here the fixation of the temporary, deformed shape is controlled by a tailored combination of thermally and strain-induced crystallization. T_{prog} was varied within ΔT_m of c(PEVA91/PEVA60) from 0 °C to 100 °C.

A three-step process was applied as the TMCP, followed by releasing the stress to zero and application of a recovery module. In Figure 1a, a typical strain–temperature–stress plot presenting the experimental data of c(PEVA91/PEVA60) programmed at T_{prog} = 75 °C and with stress-free recovery is illustrated. Cooling from T_{high} to T_{prog} (step 1) leads to a partial crystallization of the polyethylene segments under constant strain conditions, while the stress increased from an initial value σ_0 to $\sigma(T_{prog} = 75\ °C)$. After holding the sample at $\sigma(T_{prog} = 75\ °C)$ for 10 min, the stress was released again to σ_0. The deformation to ε_m at T_{prog} (step 2) increases the crystallinity caused by strain-induced crystallization. The sample was kept at ε_m and T_{prog} to allow relaxation, resulting in a decrease in stress from $\sigma(\varepsilon_m)$ to σ_m. In step 3 the sample was cooled to T_{low}, which was typically chosen to be below the onset of T_m at fixed strain (ε_m). Thermally induced crystallization of the preoriented amorphous polyethylene segments occurred, and the stress was reduced from σ_m to σ_u. After finishing the TMCP in step 4 the stress was released to

Dr. K. Kratz, Dr. S. A. Madbouly,[+] Dr. W. Wagermaier,[++]
Prof. A. Lendlein
Center for Biomaterial Development and Berlin-Brandenburg Center for Regenerative Therapies
Institute of Polymer Research
Helmholtz-Zentrum Geesthacht
Kantstr. 55, 14513 Teltow, Germany
E-mail: andreas.lendlein@hzg.de
[+] Present address: Cairo University, Faculty of Science, Department of Chemistry, 12613 Orman-Giza, Egypt
[++] Present address: Max Planck Institut of Colloids and Intrerfaces, Department of Biomaterials, 14424 Potsdam, Germany

DOI: 10.1002/adma.201102225

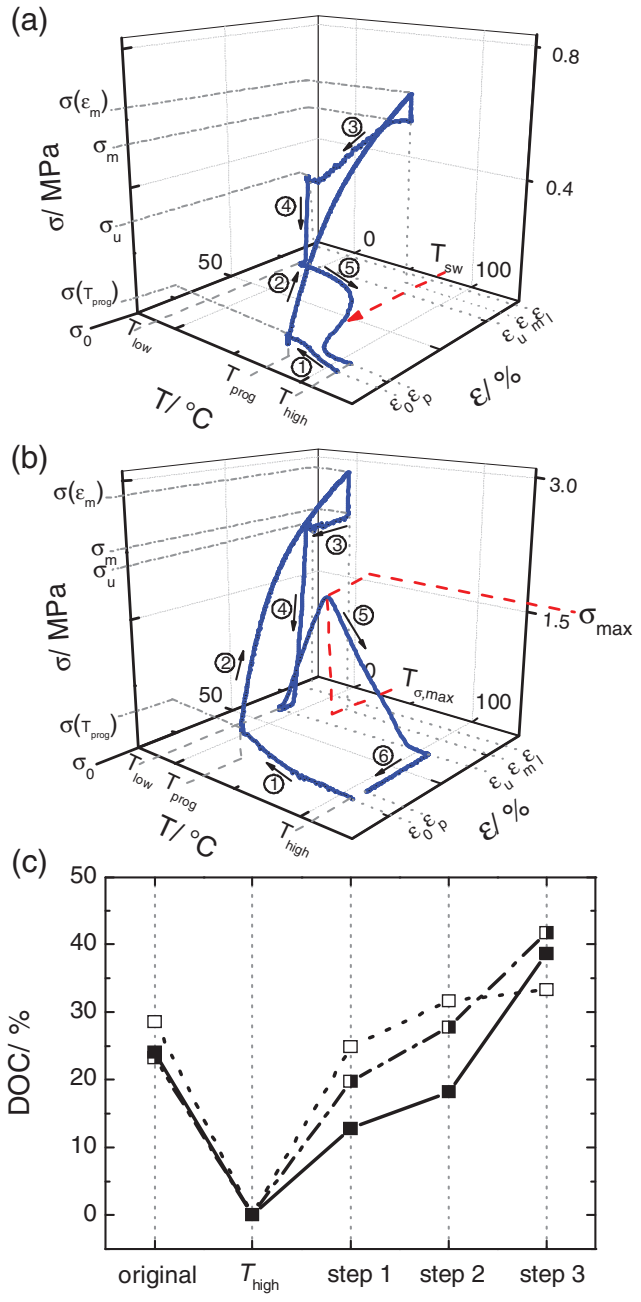

Figure 1. Examples for the cyclic thermomechanical test under stress-free and constant strain conditions as well as changes in crystallinity observed for c(PEVA91/PEVA60) during programming procedure (TMCP). a) Stress–temperature–strain plot obtained in a test protocol with stress-free recovery programmed at T_{prog} = 75 °C. Steps 1–3 represent TMCP followed by removing the stress at T_{low} (step 4), and recovery under stress-free conditions (step 5). b) Stress–temperature–strain plot obtained in a test protocol with constant strain recovery programmed at T_{prog} = 25 °C. Steps 1–3 represent TMCP followed by removing the stress to the initial value σ_0 (step 4), recovery under constant strain conditions (step 5), and removing the stress to allow recovery at T_{high} = 110 °C. c) Change in the degree of crystallinity (DOC) during TMCP programmed at T_{prog} = 25 °C (dotted line with open squares), T_{prog} = 50 °C (dashed-dotted line with half-filled squares), T_{prog} = 75 °C (solid line with filled squares) with ε_m = 75%, T_{low} = –10 °C and T_{high} = 110 °C.

σ_0, where the temporary shape (ε_u) was obtained. Finally, a stress-free recovery occurred during reheating to T_{high} resulting in the recovered strain ε_p (step 5), where T_{sw} was determined as inflection point of the strain–temperature recovery curve. In general, T_{sw} represents the temperature of maximum recovery rate (v_r).[26,36] In Figure 1b, the TME activation under constant strain conditions is displayed for a sample programmed at T_{prog} = 25 °C. After completion of TMCP (step 1–3) σ_u is achieved and in step 4 the stress is removed to σ_0. When the sample was reheated to T_{high} (step 5), σ_{max} at a temperature $T_{\sigma,max}$ was determined. In contrast to T_{sw}, $T_{\sigma,max}$ indicates the equilibrium state of the stress released by melting of the crystallites responsible for fixation of the temporary shape and the overall softening of the polymer matrix. Finally, the stress was removed to allow recovery of ε_p (step 6).

To confirm our concept for creation of TME, we explored the changes in the overall DOC at steps 1–3 during TMCP using wide-angle X-ray scattering (WAXS) experiments (see Supporting Information Method 3). After cooling from T_{high} to T_{prog} a certain DOC in the non-deformed state of the sample was obtained. The elongation of the sample at T_{prog} in step 2 resulted in an increase in the DOC caused by strain-induced crystallization followed by a thermally induced crystallization during further cooling to T_{low} (step 3). The increase in the DOC related to strain-induced crystallization (step 2) was more pronounced compared to the increase in the DOC caused by thermally induced crystallization (step 3) for lower T_{prog} (Figure 1c). At higher T_{prog} the contribution of thermally induced crystallization was predominant.

The data presented in **Figure 2** clearly demonstrate a strong correlation between the applied T_{prog} and the resulting response temperatures T_{sw} and $T_{\sigma,max}$. The strain–temperature plots of c(PEVA91/PEVA60) (Figure 2a) showed an excellent TME with high strain recovery rates R_r > 93%, while T_{sw} could be precisely controlled by variation of T_{prog} from T_{sw} = –1 °C (T_{prog} = 0 °C) up to T_{sw} = 97 °C (T_{prog} = 100 °C), with $T_{sw} \approx T_{prog}$. The shape fixity rate (R_f) was found to increase with rising T_{prog}, which was attributed to the fact that the contribution of thermally induced crystallization for fixation of the temporary shape was significantly lower at low T_{prog} compared to the situation at high T_{prog}. A small recovery temperature interval of $\Delta T_{rec} \approx$ 25 °C (particularly at low and high T_{prog}) in combination with high values for R_r > 90% was realized, as required for a wide range of industrial applications. The values obtained in the current work are superior to the data reported for an amorphous composite from polyvinyl alcohol and carbon nanotubes where ΔT_{rec} > 100 °C was required to reach only R_r = 50%.[13]

The tests performed under constant strain conditions showed an excellent TME behavior, where $T_{\sigma,max}$ increased with increasing T_{prog}, while the recovery stress σ_{max} was found to decrease (Figure 2b). $T_{\sigma,max}$ could be adjusted by variation of T_{prog} from $T_{\sigma,max}$ = 13 °C (T_{prog} = 0 °C) up to $T_{\sigma,max}$ = 102 °C (T_{prog} = 100 °C).

Multiple cyclic thermomechanical experiments resulted in both, T_{sw} as well as $T_{\sigma,max}$, being controlled systematically by variation of T_{prog} nearly independently from the thermomechanical history previous to the current programming cycle and the direction of T_{prog} variation (increasing or decreasing temperature). T_{sw} as well as $T_{\sigma,max}$ increase almost linearly with rising T_{prog} (see Figure 2c). We suggest that the slightly higher values

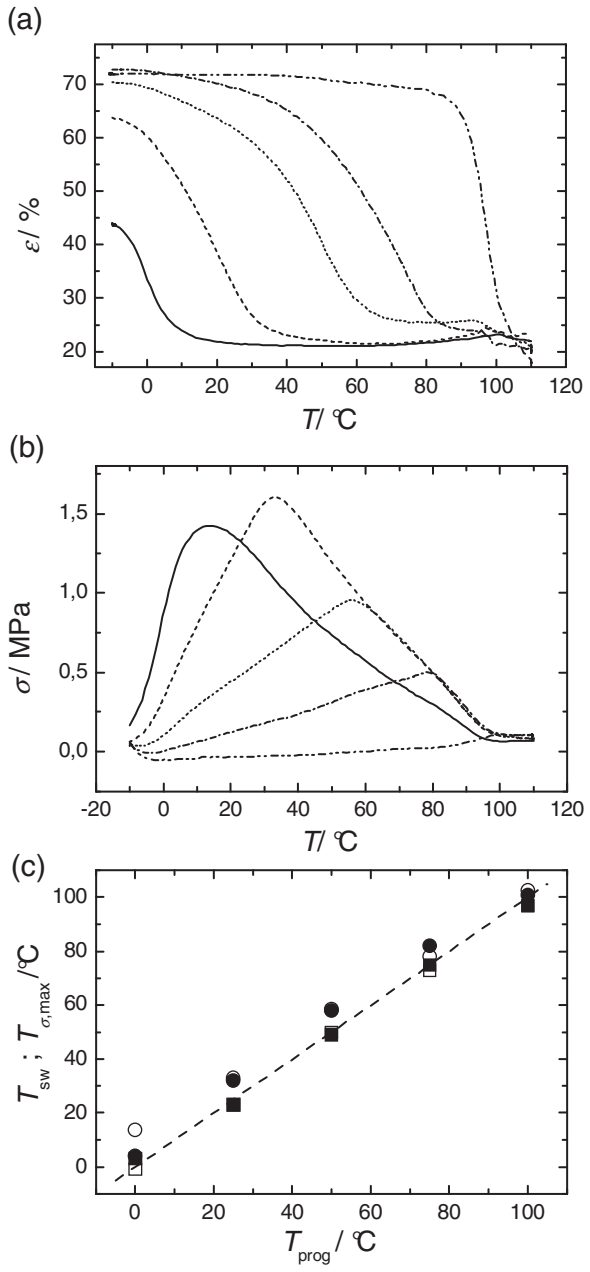

Figure 2. Temperature-memory properties of c(PEVA91/PEVA60) obtained under stress-free and constant strain conditions and relationship of the response temperatures T_{sw} and $T_{\sigma,max}$ on T_{prog}. a) Strain–temperature recovery plot; T_{prog} = 0 °C (solid line), T_{prog} = 25 °C (dashed line), T_{prog} = 50 °C (dotted line), T_{prog} = 75 °C (dash-dotted line), and T_{prog} = 100 °C (dash-double-dotted line) with T_{low} = 0 °C; T_{high} = 110 °C and ε_m = 75%. b) Stress–temperature recovery plot; T_{prog} = 0 °C (solid line), $T_{prog.}$ = 25 °C (dashed line), T_{prog} = 50 °C (dotted line), T_{prog} = 75 °C (dash-dotted line) and T_{prog} = 100 °C (dash-double-dotted line) with T_{low} = 0 °C; T_{high} = 110 °C and ε_m = 75%. c) T_{sw} and $T_{\sigma,max}$ versus T_{prog} plot. Filled squares: T_{sw} determined in five subsequent cycles with increasing T_{prog} = 0, 25, 50, 75, 100 °C; open squares: five subsequent cycles with decreasing T_{prog} = 100, 75, 50, 25, 0 °C. Filled circles $T_{\sigma,max}$ determined in five subsequent cycles with increasing T_{prog} = 0, 25, 50, 75, 100 °C; open circles: five subsequent cycles with decreasing T_{prog} = 100, 75, 50, 25, 0 °C (ε_m = 75%, T_{low} = –10 °C and T_{high} = 110 °C). The dashed trend line represents T_{sw} or $T_{\sigma,max} = T_{prog}$.

for $T_{\sigma,max}$ compared to T_{sw} obtained at the same T_{prog} originate from the different recovery mechanisms under stress-free and constant strain conditions.

To prove our concept that the realization of TME in TMPs requires an elastic polymer network with a broad ΔT_m and irregularly distributed crosslinks, we applied a TMCP to established shape-memory polymers (SMPs) with crystallizable switching segments, which did not result in a significant shift of T_{sw} when T_{prog} was varied.[27,37] We attributed the absence of a TME capability in such polymers to the relatively small ΔT_m and the homogeneity of the polymer network structure as well as the high crosslink density.

Furthermore, the feasibility of the TMP technology for potential industrial applications was explored. Self-sufficient thermoprogrammable releasing systems were investigated as example for an industrial application. Two demonstrators were fabricated from c(PEVA91/PEVA60). In **Figure 3**a–c and Supporting Information Video S1, the activation of two individual self-sufficient releasers activated at T = 47.5 °C (T_{prog} = 50 °C) and at 77.6 °C (T_{prog} = 80 °C) is shown, while in Figure 3d–f (and Supporting Information Video S2) a TME demonstrator with two different T_{sw} in one device is presented. The top fixation was released at 77 °C and the bottom fixation was unlocked at 91 °C. Finally, a TME demonstrator with three different T_{sw} could be realized in one device (Supporting Information Video S3). Three different parts of the demonstrator were programmed at three different T_{prog} = 40 °C, 60 °C, and 80 °C. When heated, three different shape changes occurred in well-separated temperature intervals (Figure 3g–j). The advantage demonstrated in these experiments, is the possibility to program the same material so that it reacts at different T_{sw}, which is quantitatively shown in Figure 2. The photoseries in Figure 3 demonstrated this programmability. In this way it is possible to change the switching series of the letters (g) to (j) be modified, which is not possible with a combination of three different dual-shape materials.

In this paper we have demonstrated that T_{sw} or $T_{\sigma,max}$ of crystallizable TMPs exhibiting a broad ΔT_m can be adjusted systematically over a wide temperature range up to 100 °C by variation of T_{prog} applied during TMCP. The broad applicability of the TMP technology was illustrated using demonstrators for thermoprogrammable self-sufficient release systems.

Experimental Section

Materials and Synthesis of TMPs: The different PEVA copolymers were named according to the ethylene content confirmed by thermogravimetric analysis (TGA) (Supporting Information Method 1). PEVA91 (91 wt% ethylene, melting index = 2.5 g per 10 min) was purchased from Polimeri Europa (product name Greenflex ML30, Milano, Italy) and PEVA60 (60 wt% ethylene, melting index = 57 g per 10 min) was obtained from DuPont de Nemours (product name Elvax40w, Neu-Isenburg, Germany). The crosslinking agent dicumyl peroxide (DCP) was purchased from Sigma-Aldrich (Sigma-Aldrich Chemie GmbH, Taufkirchen, Germany). PEVAs and DCP were used without further purification.

c(PEVA91/PEVA60) with 50 wt% PEVA91 was prepared in a two-step process. The starting materials were mixed with 0.5 wt% DCP in a twin-screw extruder Haake Minilab system Rheomex CTW5 (Thermo Electron Corporation, Newington, NH, USA) at 130 °C and a rotating speed of 50 rpm. Polymer network films of ≈1 mm thickness were obtained by compression molding in a polymer press machine type 200 E (Dr. Collin,

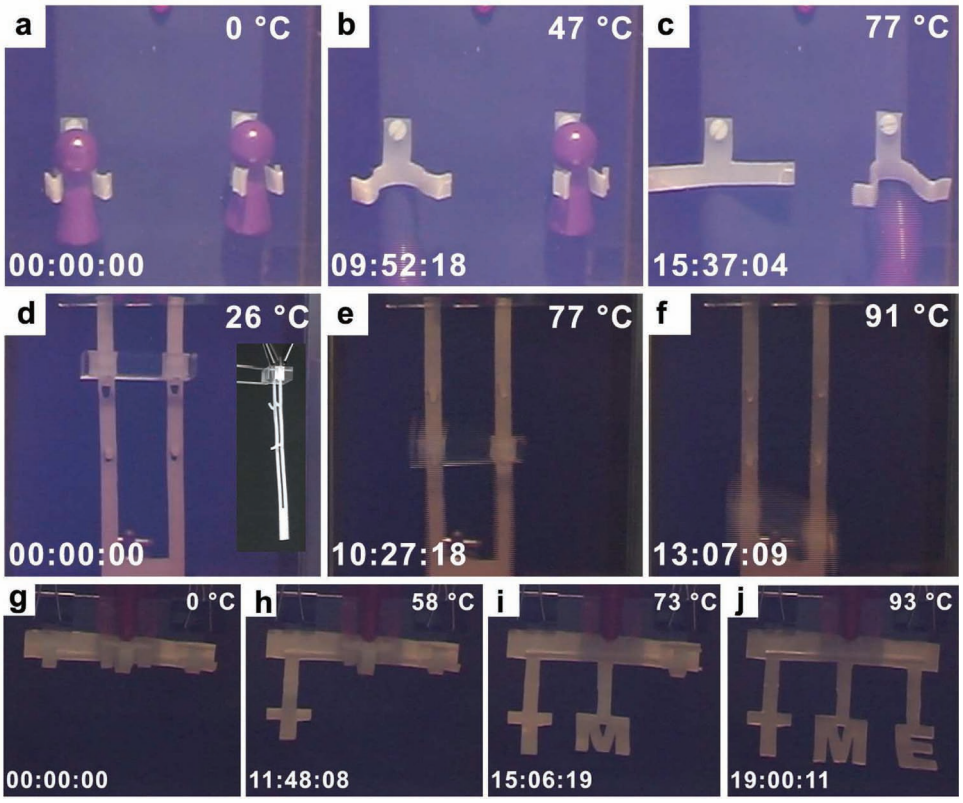

Figure 3. Photograph series of three different TME demonstration devices prepared from c(PEVA91/PEVA60). a–c) Photographs of two individual self-sufficient releasers, where one demonstrator was deformed at T_{prog} = 50 °C and the second at T_{prog} = 80 °C. The programmed devices were heated from 0 °C to 78 °C at 5 K min^{-1}. a) T = 0 °C, time t = 00:00 min; b) T = 47 °C, t = 09:52 min, left releaser is activated; c) T = 77 °C, t = 15:37 min, right releaser is activated. d–f) TME demonstrator with two different T_{sw} in one releaser, where the top fixation hooks were deformed at T_{prog} = 60 °C and the bottom fixation hooks at T_{prog} = 80 °C. The device was heated from 25 °C to 92 °C at 5 K min^{-1}. d) T = 0 °C, t = 00:00, a side view photograph of the device is also inserted; e) T = 77 °C, t = 10:27 min, release of top fixation hooks; f) T = 91 °C, t = 13:07 min, unlocking of the bottom fixation. g–j) TME shaped temperature-memory demonstrator with three different T_{sw}, here each character was deformed at a different T_{prog} = 40 °C (T), T_{prog} = 60 °C (M), and T_{prog} = 80 °C (E). Heating at 5 K min^{-1} led to three subsequent shape changes. g) T = 0 °C, t = 00:00 min; h) T = 57.7 °C, t = 11:48 min; i) T = 73.4 °C, t = 15:06 min; j) T = 93.2 °C, t = 19:00 min.

Ebersberg, Germany) at 200 °C, 90 bar. The achieved cPEVA samples were first extracted with dichloromethane. Gel content G was determined with chloroform from the ratios of the non-swollen (m_0) and extracted mass (m_e) according to $G = (m_e/m_0) \times 100$ using at least three samples.

Cyclic Thermomechanical Tensile Experiments: Experiments were performed on tensile testers Zwick Z1.0 and Z005 (Zwick, Ulm, Germany) equipped with a thermochamber and temperature controller (Eurotherm Regler, Limburg, Germany) using test specimens type 1BB (length l_0 = 20 mm, width 2 mm). Every cyclic thermomechanical experiment was preceeded by a preconditioning step, which consisted of heating the sample to T_{high}, stretching to elongation ε_m, equilibrating for 10 min, and unloading the stress to σ_0 to allow the sample to recover. This process is necessary, as a few covalent bonds can potentially break during this first deformation, which was exemplarily observed for AB- polymer networks based on poly-(ε-caprolactone) dimethacrylate as crosslinker and *n*-butyl acrylate as co-monomer.[38] After preconditioning, the sample was cooled from T_{high} to T_{prog}. Each cycle consisted of a programming module (TMCP), where the temperature-memory is created and an activation module, where T_{sw} (activation under stress-free conditions) or $T_{\sigma,max}$ (activation under constant strain conditions) was determined.

Multiple cyclic thermomechanical experiments were performed addressing five different T_{prog} (0 °C, 25 °C, 50 °C, 75 °C, and 100 °C) in subsequent cycles. These experiments were conducted using both directions: increasing and decreasing T_{prog}.

Programming Module (TMCP): The sample was cooled from T_{high} to T_{prog} and was held for 10 min. The sample was then deformed at T_{prog} to the elongation ε_m and the temperature was kept constant for 5 min to allow relaxation. Then the sample was cooled down to T_{low} under constant strain and equilibrated for 10 min. The following fixed parameters were applied (ε_m = 75%, T_{low} = –10 °C, and T_{high} = 110 °C).

Activation Under Stress-Free Conditions: The activation was induced by heating the programmed sample from T_{low} to T_{high} with a heating rate of 2 K min^{-1} under stress-free conditions. The activation module was completed by a waiting period of 10 min at T_{high}.

Activation Under Constant Strain Conditions: For the determination of the maximum stress σ_{max} and the corresponding temperature $T_{\sigma,max}$, an activation module under constant strain conditions was carried out after TMCP. The strain level was kept constant after programming and the temperature was increased from T_{low} to T_{high} with the heating rate of 2 K min^{-1}. The activation module was completed by releasing the stress to σ_0 to allow the sample to recover and a waiting period of 10 min at T_{high}.

The shape fixity rate R_f was calculated according to Equation (1) and the ability of the material to recover its original shape was quantified by the shape recovery rate R_r (Equation 2).[36]

$$R_f(N) = \frac{\varepsilon_u(N)}{\varepsilon_m} \times 100\% \quad (1)$$

$$R_r(N) = \frac{\varepsilon_u(N) - \varepsilon_p(N)}{\varepsilon_u(N) - \varepsilon_p(N-1)} \times 100\% \quad (2)$$

The experimental error and repeatability for determination of the shape-memory properties were estimated according to tested procedures, where identical protocols were applied in three repeating cycles, for T_{sw} and $T_{\sigma,max}$: ± 1 °C; σ_{max}: ± 10% of the obtained values, R_r and R_f: ± 1%.

Supporting Information

Supporting Information is available from the Wiley Online Library or from the author.

Received: June 14, 2011
Revised: July 7, 2011
Published online: August 4, 2011

[1] M. Behl, J. Zotzmann, A. Lendlein, *Adv. Polym. Sci.* **2010**, *226*, 1.
[2] T. Chung, A. Rorno-Uribe, P. T. Mather, *Macromolecules* **2008**, *41*, 184.
[3] S. Haseloh, C. Ohm, F. Smallwood, R. Zentel, *Macromol. Rapid Commun.* **2011**, *32*, 88.
[4] M. Behl, I. Bellin, S. Kelch, A. Lendlein, *Adv. Funct. Mater.* **2009**, *19*, 102.
[5] H. H. Qin, P. T. Mather, *Macromolecules* **2009**, *42*, 273.
[6] J. Zotzmann, M. Behl, D. Hofmann, A. Lendlein, *Adv. Mater.* **2010**, *22*, 3424.
[7] W. Voit, T. Ware, R. R. Dasari, P. Smith, L. Danz, D. Simon, S. Barlow, S. R. Marder, K. Gall, *Adv. Funct. Mater.* **2010**, *20*, 162.
[8] M. Behl, M. Y. Razzaq, A. Lendlein, *Adv. Mater.* **2010**, *22*, 3388.
[9] R. Vaia, J. Baur, *Science* **2008**, *319*, 420.
[10] X. Luo, P. T. Mather, *Adv. Funct. Mater.* **2010**, *20*, 2649.
[11] S. A. Madbouly, A. Lendlein, *Adv. Polym. Sci.* **2010**, *226*, 41.
[12] D. Ratna, J. Karger-Kocsis, *J. Mater. Sci.* **2008**, *43*, 254.
[13] P. Miaudet, A. Derre, M. Maugey, C. Zakri, P. M. Piccione, R. Inoubli, P. Poulin, *Science* **2007**, *318*, 1294.
[14] R. Mohr, K. Kratz, T. Weigel, M. Lucka-Gabor, M. Moneke, A. Lendlein, *Proc. Natl. Acad. Sci. USA* **2006**, *103*, 3540.
[15] U. Narendra Kumar, K. Kratz, W. Wagermaier, M. Behl, A. Lendlein, *J. Mater. Chem.* **2010**, *20*, 3404.
[16] I. Bellin, S. Kelch, A. Lendlein, *J. Mater. Chem.* **2007**, *17*, 2885.
[17] T. Takahashi, N. Hayashi, S. Hayashi, *J. Appl. Polym. Sci.* **1996**, *60*, 1061.
[18] M. Behl, A. Lendlein, *J. Mater. Chem.* **2010**, *20*, 3335.
[19] I. Bellin, S. Kelch, R. Langer, A. Lendlein, *Proc. Natl. Acad. Sci. USA* **2006**, *103*, 18043.
[20] J. Li, T. Xie, *Macromolecules* **2011**, *44*, 175.
[21] Z. He, N. Satarkar, T. Xie, Y.-T. Cheng, J. Z. Hilt, *Adv. Mater.* **2011**, *23*, 3192.
[22] I. S. Kolesov, H.-J. Radusch, *Express Polym. Lett.* **2008**, *2*, 461.
[23] L. Sun, W. M. Huang, *Soft Matter* **2010**, *6*, 4403.
[24] T. Xie, *Nature* **2010**, *464*, 267.
[25] B. K. Kim, S. Y. Lee, M. Xu, *Polymer* **1996**, *37*, 5781.
[26] I. S. Kolesov, K. Kratz, A. Lendlein, H. J. Radusch, *Polymer* **2009**, *50*, 5490.
[27] P. Ping, W. S. Wang, X. S. Chen, X. B. Jing, *Biomacromolecules* **2005**, *6*, 587.
[28] J. Cui, K. Kratz, M. Heuchel, B. Hiebl, A. Lendlein, *Polym. Adv. Technol.* **2011**, *22*, 180.
[29] J. Cui, K. Kratz, A. Lendlein, *Smart Mater. Struct.* **2010**, *19*.
[30] T. Xie, K. A. Page, S. A. Eastman, *Adv. Funct. Mater.* **2011**, *21*, 2057.
[31] A. Arsac, C. Carrot, J. Guillet, *J. Appl. Polym. Sci.* **1999**, *74*, 2625.
[32] M. Brogly, M. Nardin, J. Schultz, *J. Appl. Polym. Sci.* **1997**, *64*, 1903.
[33] Y. T. Sung, C. K. Kum, H. S. Lee, J. S. Kim, H. G. Yoon, W. N. Kim, *Polymer* **2005**, *46*, 11844.
[34] S. Bistac, P. Kunemann, J. Schultz, *Polymer* **1998**, *39*, 4875.
[35] F. K. Li, W. Zhu, X. Zhang, C. T. Zhao, M. Xu, *J. Appl. Polym. Sci.* **1999**, *71*, 1063.
[36] W. Wagermaier, K. Kratz, M. Heuchel, A. Lendlein, *Adv. Polym. Sci.* **2010**, *226*, 97.
[37] H. A. Khonakdar, S. H. Jafari, S. Rasouli, J. Morshedian, H. Abedini, *Macromol. Theory Simul.* **2007**, *16*, 43.
[38] A. Lendlein, A. M. Schmidt, R. Langer, *Proc. Natl. Acad. Sci. USA* **2001**, *98*, 842.